JOURNAL OF APPLIED ELECTROCHEMISTRY **22** (1992) 506–511

Voltammetric study of plating baths for electrodeposition of Co–W amorphous alloys

K. WIKIEL, J. OSTERYOUNG

Department of Chemistry, State University of New York at Buffalo, Buffalo, New York 14214, USA

Received 7 March 1991; revised 12 September 1991

Cyclic voltammetry and chronoamperometry at glassy carbon and platinum microdisc electrodes have been used to study the electrodeposition of Co–W amorphous alloys. Voltammetric results show that cathodic deposition of Co–W alloy is accompanied by hydrogen evolution and the efficiency of Co–W electrodeposition does not exceed 20%. Voltammetric behaviour of cobalt (II) and tungstate in ammonium citrate solution depend strongly on composition of the plating bath. The concentration of Co(II) ions can be monitored *in situ* during electroplating by means of anodic stripping voltammetry at a platinum microelectrode. The deposit of the alloy on the microelectrode is stable in the atmosphere and thus can be stored for subsequent comparison with a deposit obtained later in the life of the working bath.

1. Introduction

Amorphous alloys show some remarkable properties. Some of them have special magnetic characteristics, small temperature coefficient of linear expansion and low electrical resistivity [1, 2]. Glassy alloys can be made extremely hard and highly wear resistant. They have relatively homogeneous surface compared to their crystalline counterparts, and this has sometimes been used to explain high resistance to localized corrosion attack [3, 4]. Glassy alloys are usually produced by rapid solidification of liquid components, but thin layers of such alloys can be formed also by electrodeposition [5–10]. Electrodeposited Co–W amorphous alloy can provide high surface hardness with good ductility and excellent corrosion resistance [5].

A previous paper dealt with the anodic decomposition of electrolytes for plating of Co–W and Ni–W amorphous alloys [11]. The overall objective of the work presented here is to devise a method for characterizing the electroplating bath for electrodeposition of Co–W and for monitoring the electrochemical reactivity. Voltammetric and potential step transient methods at microelectrodes were chosen to investigate the system because small electrodes decrease effects of uncompensated *IR* drops, even at very high current densities, decrease charging currents, and enhance mass transport by diffusion. These properties make it possible to work at the high concentrations associated with plating processes and to obtain currents controlled by diffusion in the presence of convective mass transport. The usefulness of microelectrodes in this type of study has been shown by Howarth and Pletcher [12]. They studied a simpler system in which only one component of the plating bath (chromium(III)) was deposited.

2. Experimental details

EG&G PARC Lot No. 100 Pt (platinum) and No. 3989 GC (glassy carbon) microdisc electrodes were used. The nominal radius of these electrodes is $5\,\mu$m. The microdisc electrodes were polished before use with carbimet sandpaper of decreasing grit size and subsequently with Microcloth polishing cloth with suspensions of alumina powder (Buehler Ltd) down to $0.05\,\mu$m. Electrodes were lightly repolished before each experiment. The quality of the surface was checked optically with 500 × magnification (Leitz-Dievert microscope). The reference electrode was saturated calomel (SCE), and all potentials are quoted with respect to this. A platinum counter electrode ($A = 2\,\mathrm{cm}^2$) was used.

An IBM-type jacketed three-electrode cell was used. The temperature of solutions was controlled by using a GCA Circulation System-250.

All cyclic voltammetric and anodic stripping experiments were carried out using an EG&G PARC 173 potentiostat equipped with an EG&G PARC 179 coulometer, an EG&G PARC 175 universal programmer and a Houston Instruments 2000 XY recorder. Chronoamperometric data were collected using a DEC PDP 8/e laboratory minicomputer interfaced with an EG&G PARC Model 273 pontentiostat.

All reagents were of analytical grade, and distilled water passed through a four-cartridge Millipore Milli-Q purification system was used for preparation of the solutions. Purified argon was used for deoxygenation.

The plating bath for electrodeposition of Co–W amorphous alloys was prepared according to the patent description [5]. The term 'plating bath' is used to refer to the basic bath composition, that is, 0.26 M $(NH_4)_2$ cit. + 0.165 M BPO_4 + 0.25 M Na_2WO_4 +

0021-891X/92

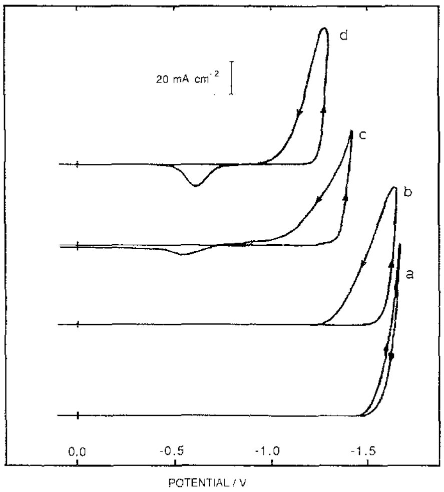

Fig. 1. Cyclic voltammograms obtained on glassy carbon microdisc electrode in deoxygenated solution of: (a) 0.26 M $(NH_4)_2$cit. + 0.165 M BPO_4, pH 9.2; (b) a + 0.25 M Na_2WO_4; (c) a + 1.3 × 10^{-2} M Co(II); (d) a + 0.25 M Na_2WO_4 + 1.3 × 10^{-2} Co(II). Scan rate 50 mV s^{-1}.

1.3 × 10^{-2} M $Co(SO_4)$, with NH_3(aq) added to bring the pH to 9.2 at 25° C. This composition yields deposits of Co–W amorphous alloy of approximate cobalt-to-tungsten ratio 1 : 1 by weight (3 : 1 atom ratio). Minor amounts of boron and phosphorous are also present. The composition of the alloy was determined by energy-dispersive X-ray (EDAX) analysis of the deposits and by a bulk analysis whereby amorphous films were deposited on copper coupons, dissolved electrolytically into ammonium citrate solution, and the resulting solutions analysed by inductively coupled plasma-atomic emission spectrometry (ICP-AES). The amorphous nature of the alloys was verified by X-ray diffraction.

3. Results and discussion

3.1. *Cyclic voltammetry*

The first series of experiments was performed in deoxygenated solutions of plating bath. Figure 1 shows typical cyclic voltammograms obtained at a glassy carbon microdisc electrode with a wide range of potential limits. Voltammogram 1A was obtained in a solution of ammonium citrate and boron phosphate. Only the hydrogen evolution process, starting around -1.5 V, was observed. According to Wiart [13], in such solutions (pH > 8) protons are not likely to be reduced; however citrate can probably release the labile hydrogen of the alcohol functional group. At lower current sensitivity a poorly defined limiting current is observed for this part of the voltammogram at glassy carbon microelectrodes. This would support this hypothesis. On the other hand, the value of limiting current density (about 4 A cm^{-2}) is larger than the predicted steady-state current density for such a reaction (*ca.* 1.1 A cm^{-2}).

The remaining three voltammograms (curves 1b–d), though different, show three main features: (a) virtually zero cathodic current on the forward scan until the onset of a nucleation process; (b) a rapid rise of the current on the forward scan; (c) crossover between anodic and cathodic current after reversing the sweep. Voltammogram 1b was obtained in a solution containing tungstate. Although the direct reduction of tungstate to metallic tungsten is impossible under these conditions [14], a strong hysteresis indicates some changes on the electrode surface. Such changes can be caused by reduction of WO_4^{2-} to form insoluble tungsten oxides, such as WO_2. It has been reported [15] that during the electrolysis of tungsten-containing electrolytes, slightly soluble intermediates are formed on the cathode. Moreover, tungsten intermediates act as hydrogen evolution catalysts, which can explain the hysteresis in the voltammogram. The formation of MoO_2 during the electrolysis of molybdate-containing citrate electrolytes has been reported also [13].

When cobalt(II) is present instead of tungstate (curve c, Fig. 1) the cathodic current starts to rise at a potential about 200 mV more positive than in curves a and b. The shift of the rising part of the forward scan, a strong hysteresis and a small anodic peak suggest that a new phase is deposited on the glassy carbon surface. The appearance of the anodic peak at potential about -0.6 V suggests that metallic cobalt is electrodeposited, but comparison of cathodic and anodic charges indicates that hydrogen evolution remains the main cathodic process in this system.

Finally, Fig. 1d shows the response from the same experiment as above but with both cobalt(II) and tungstate present. This solution corresponds to the full plating bath composition (without additives). The voltammogram, curve 1d, is similar to the previous one (1c), but the rising portion of the cathodic current occurs at a potential about 100 mV more positive, and the anodic peak observed during the reverse scan is larger and better shaped than before. It is not obvious whether the anodic peak corresponds to the oxidation of electrodeposited Co–W or metallic cobalt, electrodeposition of which is catalysed by the presence of tungstate. In order to answer this question large scale electrodeposition was carried out on a Cu coupon and the resulting deposit was dissolved electrolytically. The results of ICP-AES analysis of this final solution confirmed that the anodic peak of Fig. 1d corresponds to the oxidation of Co–W alloy.

Figure 2 presents the results of experiments analogous to those of Fig. 1, but at a platinum microdisc electrode. The main difference between the behaviour of these two electrode materials is in the difference in overvoltage for hydrogen evolution. Voltammograms 2a and 2b are virtually the same, though curve 2b was obtained with tungstate present. Despite the results obtained at the glassy carbon electrode, the formation of tungsten intermediates is not observed on platinum, because of competitive hydrogen evolution occuring at far lass negative potential. If Co(II) is present (curve 2c), the rate of hydrogen evolution is decreased. This effect is even more marked in the full plating bath (Co(II) and tungstate both present, voltammogram 2d). In contrast with the results at glassy carbon, no hysteresis is observed at the platinum electrode. Thus the

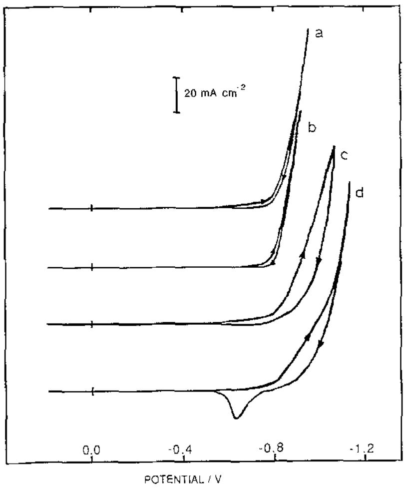

Fig. 2. Cyclic voltammograms on platinum microelectrode. Conditions and solutions as in Fig. 1.

overvoltage for hydrogen evolution on the gradually forming new phase of Co–W is markedly higher (more negative) than on the bare platinum surface. A very well shaped anodic peak for oxidation of Co–W is observed in Fig. 2d.

Similar experiments, like those described above, were performed at various temperatures within the range of 25–65° C. The changes of temperature did not change the general voltammetric characteristics of the system, and no new features were observed.

3.2. *Chronoamperometric transients*

Figure 3 presents chronoamperometric responses to potential steps from 0.0 V obtained at a glassy carbon microelectrode. A smoothly rising transient following an initial delay is observed up to 20 s. After that time a rather erratic response is observed for the more negative steps. The observed current reflects two processes, namely growth of a new phase (i.e. the Co–W alloy) and hydrogen evolution. Since hydrogen evolution occurs only on a continually deposited alloy, the total current is strictly proportional to the current for deposition of the alloy, at least when the curve is smooth, and therefore the hydrogen evolution reaction does not change the shape of the *i–t* response.

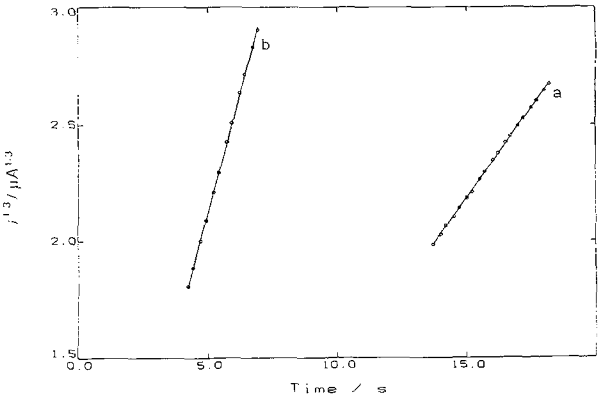

Fig. 4. $I^{1/3}$ against time plot for the rising portion of curves a and b in Fig. 3.

The first part of the rising portions of curves a and b of Figure 3 show very good linear dependence of $I^{1/3}$ on time as shown in Fig. 4. This type of dependence is consistent with the model of progressive nucleation and three-dimensional growth [16]. The analysis of the first part of curve 3c shows, rather, linear dependence of $I^{1/2}$ on time, which indicates the transition to instantaneous nucleation followed by three-dimensional growth.

Figure 5 presents chronoamperometric responses for similar experiments at a platinum microelectrode. Again, due to the lower hydrogen overvoltage, potential step responses look markedly different from those at glassy carbon. Instead of the initial delay, an initial decay of current followed by gradual increase is observed. Again it follows that there is a competition between hydrogen evolution and deposition of new phase onto the platinum surface. Due to the changing rate of hydrogen evolution, the rising portion of the chronoamperometric current does not have a simple fractional power dependence on time.

Comparing the chronoamperometric results obtained at glassy carbon and platinum microelectrodes, notice that the erratic response occurs at platinum for a much more negative potential step. This is somewhat surprising, because this kind of behaviour is explained by the formation of insoluble hydroxy precipitates of deposited metal [12]. The increase of the concentration

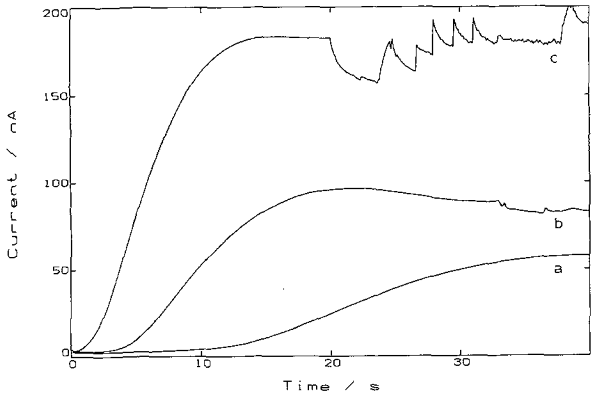

Fig. 3. Chronoamperometric responses to potential steps from 0.0 V to *E*/V: (a) −0.95; (b) −0.97; (c) −1.0. Glassy carbon microelectrode in a solution of plating bath at 65° C.

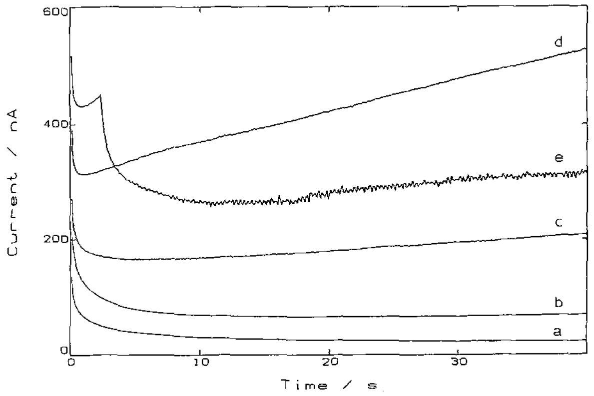

Fig. 5. Chronoamperometric responses to potential changes from 0.0 V to *E*/V: (a) −0.94; (b) −0.98; (c) −1.02; (d) −1.06; (e) −1.08. Platinum microelectrode in a solution of plating bath at 65° C.

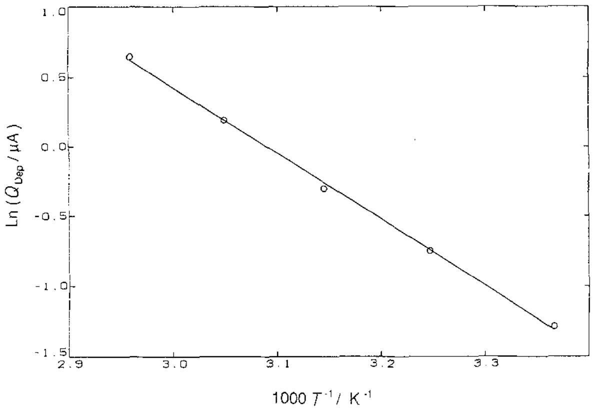

Fig. 6. Arrhenius-type plot for deposition of Co–W alloy at a platinum microelectrode. Q_{dep} is the charge corresponding to deposition at -1.0 V for 60 s.

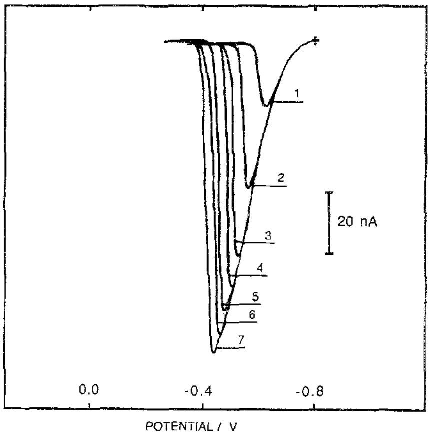

Fig. 7. Anodic stripping voltammograms for various concentration of Co(II) in plating bath. Platinum microelectrode. Deposition potential -1.1 V; deposition time 60 s; scan rate 50 mV s^{-1}; temperature 25° C. Concentration of Co(II)/mM: (1) 1, (2) 2, (3) 4, (4) 6, (5) 8, (6) 12, (7) 16.

of hydroxide ion in the vicinity of the electrode surface is caused by the hydrogen evolution process [12]. In the present case, the overvoltage for the hydrogen evolution reaction is definitely less negative at the platinum surface, so also the changes in pH at the electrode surface should be larger at this electrode at a given potential. But the results display just the opposite behaviour, so it follows that something else causes the erratic responses, and that hydrogen evolution can even shift to more negative values the potential at which the noisy chronoamperometric transient begins.

3.3. *Activation energy for deposition*

Figure 6 presents an Arrhenius-type of plot for electrodeposition of the Co–W alloy at a platinum microelectrode. The rate of deposition was measured by the oxidation charge after a 60 s step to -1.0 V. This method allowed us to eliminate the current connected with the hydrogen evolution process. (The results are markedly more reproducible on platinum than on glassy carbon; apparently the deposit interacts more strongly with the glassy carbon substrate). Results obtained over the temperature range of 24 to 60° C give a fairly good linear Arrhenius-type plot. The value of 39 kJ mol^{-1} calculated as an activation energy from the slope is too large for a simple diffusion-controlled process and suggests, rather, kinetically controlled electrodeposition. (Of course, we do not know what the reaction is; the activation energy is perhaps better expressed as kJ (unit $reaction)^{-1}$).

3.4. *Anodic stripping voltammetry*

It was noticed during the cyclic voltammetric experiments that the shape of the cyclic curves depends on composition of the plating bath. The height of the very well defined anodic peak corresponding to electrooxidation of Co–W strongly depends on the concentration of Co(II) in the plating bath. Since electrodeposition of Co–W alloy is performed with insoluble anodes, the Co(II) concentration is 20 times smaller than the concentration of tungstate, and the mole ratio of Co to W is 3 : 1, it is very important to monitor depletion of the Co(II) concentration in the working bath during electroplating. Figure 7 shows typical anodic stripping voltammograms obtained at the platinum microelectrode in the plating bath with various concentrations of Co(II). It should be stressed, once again, that the anodic stripping peak at the platinum electrode was definitely better shaped and more reproducible than at the glassy carbon microelectrode. Figure 8 presents corresponding calibration curves. Figure 8a shows very strong dependence of the height of stripping peak on Co(II) concentration within the range of 1–6 mM and then the tendency to form a plateau, because of broadening of the peak with increasing concentration of Co(II). This effect is less visible in curve 8b, representing the anodic peak charge versus Co(II) concentration.

It should be stressed that the anodic stripping peak does not depend on changes in tungstate concentration within the range 0.1–0.25 M. This is as expected, for the mole ratio of tungsten to cobalt is so much larger in the solution than in the alloy.

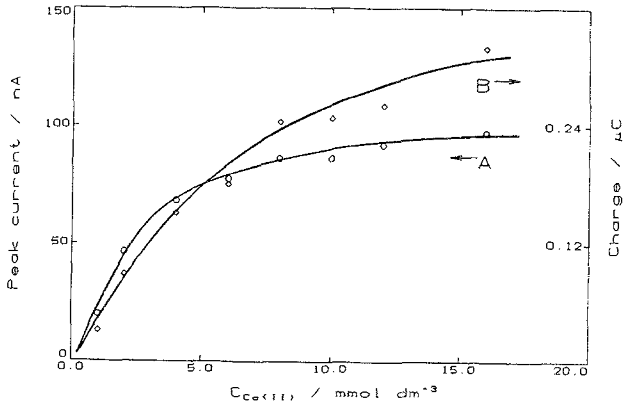

Fig. 8. Calibration curves for Co(II) concentration in plating bath. Conditions as in Fig. 7. A — Anodic stripping peak current. B — Anodic stripping peak charge.

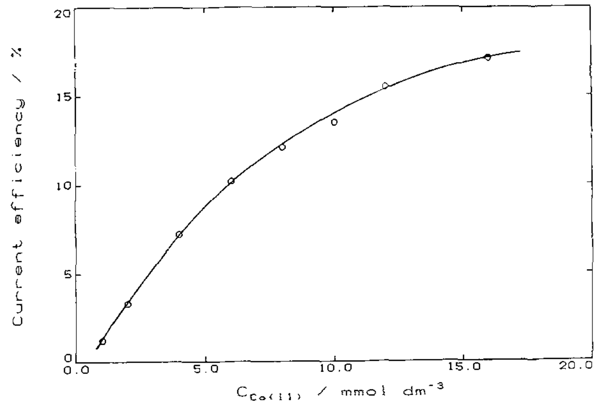

Fig. 9. The influence of Co(II) concentration on current efficiency for Co–W electrodeposition on platinum microelectrode at 65° C.

Figure 9 presents the dependence of current efficiency (the ratio of anodic stripping peak charge to the total deposition charge) on concentration of cobalt in the plating bath. This plot was obtained at 65° C at a platinum electrode, and it means that, even under conditions close to the real operating conditions, the current efficiency for the nominally full plating bath composition is slightly less than 20%, and that the hydrogen evolution reaction remains the main cathodic process.

Anodic stripping results presented above indicate that this method could be employed successfully to *in situ* monitoring of the Co(II) concentration. The special features of the diffusion field at a microelectrode make it possible to work under anodic stripping conditions without stirring. The very small size of a possible monitoring device based on such an electrode make such a project even more attractive. Moreover, according to the results presented in Fig. 9, also current efficiency can be employed to estimate cobalt concentration in the plating bath.

3.5. *The deposit as a record*

Because of the extremely good resistance of the Co–W alloy to chemical attack, it was very interesting to see if it is possible to store a 'finger print' of a properly working electroplating bath, that is, a deposit of an alloy on a platinum microelectrode. In a research setting, according to the results presented, concentration of Co or plating efficiency can be determined by anodic stripping voltammetry. The stripping step and the associated analysis and interpretation of data are the complex part of this experiment, whereas the plating step is quite simple and could be automated readily for implementation in a working bath. If deposits can be obtained routinely and stored without deterioration, they can be examined as needed by a trained person in a laboratory setting to monitor the condition of the bath.

Figure 10 presents anodic stripping voltammograms obtained in a plating bath. The deposition step for all of them was performed in the same freshly prepared electroplating solution, but after that the electrodes (with their deposits) were stored (exposed to the atmosphere) for various periods of time. Curve 3 in Fig. 10 is an anodic stripping voltammogram obtained 3 days after electrodeposition of the Co–W alloy. The shape of this voltammogram is almost the same, and the height of the anodic peak is only slightly lower than that for the freshly deposited and immediately stripped Co–W alloy (curve 1 in Fig. 10). Thus the stored deposit from the initial bath provides a standard for subsequent investigation of the reactivity of the working bath during the plating process.

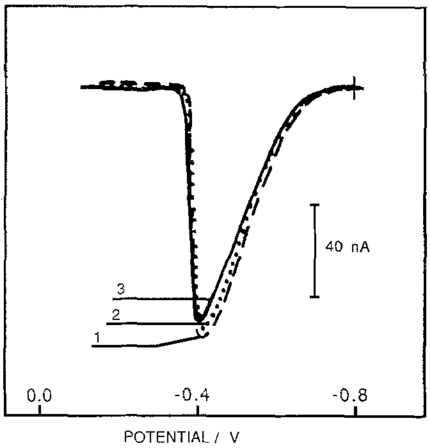

Fig. 10. Anodic stripping voltammograms obtained in plating bath. Stripping step: (1) immediately; (2) 1 day; (3) 3 days after deposition of Co–W. Platinum microelectrode in plating bath. Deposition potential −1.1 V; deposition time 60 s; scan rate 50 mV s^{-1}; temperature 25° C.

Acknowledgements

The authors are grateful to Eugene Lunghofer and Larry Wolfe for helpful discussion, to Mikolaj Donten for technical assistance and to the New York State Science and Technology Foundation (RDG 81964) for financial support in cooperation with EPL, Inc. and AMTECH.

References

[1] F. E. Luborsky, ed., 'Amorphous Metallic Alloys', Butterworths, London (1983).

[2] S. R. Nagel, 'Advanced Chemical Physics, I', (edited by Prigogne and S. A. Rice) vol. 5, Wiley, New York (1982), pp. 227–75.

[3] M. D. Archer, C. C. Corke and B. H. Harji, *Electrochim. Acta* **32** (1987) 13.

[4] P. C. Searson, P. V. Nagaskar and R. M. Latanision, in 'Modern Aspects of Electrochemistry', (edited by R. E. White, J. O'M. Bockris and B. E. Conway), vol. 21, Plenum Press, New York (1990), pp. 121–61.

[5] G. A. Croopnick and D. M. Scruggs, *US patent* 4 529 668 (1985).

[6] T. Omo, H. Yamamoto and H. L. Glass, *J. Electrochem. Soc.* **119** (1972) 168.

[7] T. Watanabe, *New Materials New Processes* **3** (1985) 307.

[8] M. Ogata, *Kinzoku Hyomen Gijutsu* **39** (1988) 169; *CA* **109**: 13505n.

[9] T. Watanabe, *Hyomen Gijutsu* **40** (1989) 375; *CA* **110**: 197365s.

[10] A. Budniok and J. Kupka, *Electrochim. Acta* **34** (1989) 871.

[11] M. Donten and J. Osteryoung, *J. Appl. Electrochem.* **21** (1991) 496.

[12] J. N. Howarth and D. Pletcher, *ibid.* **18** (1989) 644.

[13] E. Chassing, K. Vu Quang and R. Wiart, *ibid.* **18** (1989) 839.

[14] A. T. Vas'ko, 'Encylopedia of Electrochem. of Elements', (edited by A. J. Bard), vol. 5, Marcel Dekker, New York (1976).

[15] A. T. Vas'ko, 'Standard Potential in Aqueous Solution', (edited by A. J. Bard, R. Parsons, and J. Jordon), Marcel Dekker, New York (1985), p. 486.

[16] J. N. Howarth and D. Pletcher, *J. Chem. Soc. Faraday Trans.* **I83** (1987) 2787.